Human Molecular Genetics, 2021, Vol. 30, No. 22 2053–2067

https://doi.org/10.1093/hmg/ddab169
Advance Access Publication Date: 24 June 2021
General Article

GENERAL ARTICLE

Prenatal inflammation as a link between placental expression signature of tryptophan metabolism and preterm birth

Rona Karahoda[1], Morgane Robles[2], Julia Marushka[3], Jaroslav Stranik[4], Cilia Abad[1], Hana Horackova[1], Jurjen Duintjer Tebbens[3], Cathy Vaillancourt[2], Marian Kacerovsky[4] and Frantisek Staud[1,*,†]

[1]Department of Pharmacology and Toxicology, Faculty of Pharmacy in Hradec Kralove, Charles University, Hradec Kralove 50005, Czech Republic, [2]INRS-Centre Armand-Frappier Santé Biotechnologie, Laval, QC H7V 1B7, Canada, [3]Department of Biophysics and Physical Chemistry, Faculty of Pharmacy in Hradec Kralove, Charles University, Prague 50005, Czech Republic and [4]Department of Obstetrics and Gynecology, University Hospital Hradec Kralove, Hradec Kralove 50005, Czech Republic

*To whom correspondence should be addressed. Tel: +420 495067407; Email: frantisek.staud@faf.cuni.cz

Abstract

Spontaneous preterm birth is a serious medical condition responsible for substantial perinatal morbidity and mortality. Its phenotypic characteristics, preterm labor with intact membranes (PTL) and preterm premature rupture of the membranes (PPROM), are associated with significantly increased risks of neurological and behavioral alterations in childhood and later life. Recognizing the inflammatory milieu associated with PTL and PPROM, here, we examined expression signatures of placental tryptophan metabolism, an important pathway in prenatal brain development and immunotolerance. The study was performed in a well-characterized clinical cohort of healthy term pregnancies ($n = 39$) and 167 preterm deliveries (PTL, $n = 38$ and PPROM, $n = 129$). Within the preterm group, we then investigated potential mechanistic links between differential placental tryptophan pathway expression, preterm birth and both intra-amniotic markers (such as amniotic fluid interleukin-6) and maternal inflammatory markers (such as maternal serum C-reactive protein and white blood cell count). We show that preterm birth is associated with significant changes in placental tryptophan metabolism. Multifactorial analysis revealed similarities in expression patterns associated with multiple phenotypes of preterm delivery. Subsequent correlation computations and mediation analyses identified links between intra-amniotic and maternal inflammatory markers and placental serotonin and kynurenine pathways of tryptophan catabolism. Collectively, the findings suggest that a hostile inflammatory environment associated with preterm delivery underlies the mechanisms affecting placental endocrine/transport functions and may contribute to disruption of developmental programming of the fetal brain.

†Frantisek Staud, http://orcid.org/0000-0001-6712-097X
Received: May 13, 2021. **Revised:** June 16, 2021. **Accepted:** June 17, 2021

Introduction

Preterm birth is defined as delivery before 37 weeks of gestation, and the latest data (from 2014) indicate an incidence of 10% of live births globally (1). Two main categories of preterm birth are iatrogenic (health provider–initiated) preterm delivery and spontaneous preterm birth. The latter may further be categorized as labor with intact membranes (hereafter PTL) or preterm premature rupture of membranes (PPROM) (2). Although the etiology remains unclear, multiple mechanisms have been related to spontaneous preterm delivery, including prenatal infection/inflammation, vascular disorders, breakdown of maternal–fetal tolerance and stress (2,3). Preterm delivery is also often complicated by the presence of microbial invasion of amniotic cavity (MIAC) and/or intra-amniotic inflammation (IAI), or subsequently histological chorioamnionitis (HCA), further contributing to the pathogenesis (4).

Importantly, preterm births are associated with approximately 75% of perinatal mortality cases and increased long-term morbidity (2). Of particular concern are strong associations with diverse neurodevelopmental, psychiatric, cognitive and behavioral sequelae, including cerebral palsy, mental and cognitive deficits, sensory impairments, attention deficit hyperactivity disorder, schizophrenia, autism spectrum disorder and epilepsy (5,6). In response to stressful stimuli, intrauterine programming of neurological processes is now recognized as the prime modulator predisposing the developing fetus to adult-onset disease. As a central element of the maternal–fetal interface, the placenta has been shown to play a crucial role in feedback responses to pathological insults, and thus developmental origins of disease (7). By investigating the transcriptional differences between term and preterm placentas, we may help identify mechanisms contributing to preterm etiology and long-term consequences.

In recent years, placental catabolism of L-tryptophan has been identified as a plausible mechanistic link between disturbance of the prenatal environment and predisposition to mental health disorders in later life (8,9). In the placenta, tryptophan is metabolized via the serotonin and kynurenine pathways, generating metabolites with neuroactive, immunosuppressive, vasoactive and redox properties (10–12). Tryptophan homeostasis in the fetoplacental unit is fine-tuned by a network of genes, protein and transcription factors (13) and is crucial for proper placental function, fetal development and programming. However, several pathological conditions, including inflammation (14,15), preeclampsia (16–19), fetal growth restriction (20,21) and gestational diabetes (22), affect the expression and activity of enzymes involved in tryptophan metabolism and thus may disturb tryptophan metabolite levels in the fetoplacental unit and affect pregnancy outcomes.

A large body of evidence has characterized the kynurenine pathway as particularly susceptible to immune activation and stress, which reportedly induce increases in levels of kynurenine metabolites in the fetal brain following perinatal exposure (23,24). Moreover, the expression of several kynurenine pathway enzymes is upregulated in placentas exposed to infection, ultimately leading to neurotoxic quinolinic acid (QUIN) production and increased levels of QUIN in cord blood (15). Equally significant, maternal inflammation reportedly upregulates placental serotonin synthesis in mice (25). Understanding these alterations and modifications is crucial as disturbance of the serotonin balance in pregnancy has been shown to be embryotoxic and teratogenic (26).

Recognizing the hostile *in utero* environment associated with PTL and PPROM, an intuitive hypothesis is that tryptophan metabolism may be transcriptionally altered in placentas from preterm birth. To test this hypothesis and determine the nature and extent of these alterations, we analyzed the expression of relevant genes in a well-characterized cohort of term ($n = 39$) and preterm ($n = 167$) placentas. Using robust statistical analysis, we reveal putative relationships between maternal inflammation, preterm delivery, the placental tryptophan pathway and gestational age at delivery. Elucidating these associations will help efforts to understand the complex processes linking maternal/intrauterine inflammatory events and poor neurodevelopmental outcomes.

Results

Characteristics of the cohort

Table 1 shows the demographic and clinical characteristics of pregnant women ($n = 206$) enrolled in this study. Samples were divided into placentas from term ($n = 39$), PTL ($n = 38$) and PPROM ($n = 129$) pregnancies. As per definition, significant differences were observed in gestational ages at sampling and delivery, and birth weight between term, PPROM and PTL deliveries ($q \leq 0.001$). Moreover, BMI at admission was significantly higher for the term group than the PTL group ($q = 0.0332$). No significant between-group differences in fetal sex distribution were detected. Preterm deliveries were associated with administration of corticosteroids, antibiotics and tocolytics. Within the preterm group, PTL samples were associated with significantly higher amniotic fluid IL-6 levels at admission ($q = 0.0060$; Roche dataset) and maternal serum CRP concentration at delivery ($q = 0.0075$), compared with PPROM.

Placental expression of tryptophan pathway genes differs between preterm births and term deliveries

As shown in Figure 1, there were significant differences in gene expression between the preterm and term placentas. Thirteen genes encoding enzymes involved in the serotonin and kynurenine metabolic pathways and three encoding tryptophan and serotonin transporters were analyzed. Evaluation of the expression of two, *ASMT* and *TPH2*, by qPCR analysis was restricted by the detection limits, a feature independent of the clinical categorization. The expression of 12 genes significantly differed between preterm and term placentas. Relative expression of two kynurenine pathway genes was significantly upregulated in placentas from preterm births compared with placentas from term deliveries—*IDO1* ($\log2(FC) = 1.37$, $q < 0.0001$) and *HAAO* ($\log2(FC) = 0.26$, $q < 0.01$)—and expression of one (*KYNU*: $\log2(FC) = -0.51$, $q < 0.001$) was downregulated (Fig. 1A). The serotonin pathway (Fig. 1B) was more strongly affected. Relative expression of three genes of this pathway was upregulated in preterm placentas: *PTS* ($\log2(FC) = 0.91$, $q < 0.0001$), *SPR* ($\log2(FC) = 2.12$, $q < 0.0001$) and *MAOB* ($\log2(FC) = 0.72$, $q < 0.01$). In addition, three of the genes were significantly downregulated: *ASMT* ($\log2(FC) = -1.82$, $q < 0.0001$), *TPH2* ($\log2(FC) = -0.94$, $q < 0.05$) and *MAOA* ($\log2(FC) = -0.15$, $q < 0.05$) in preterm placentas. Relative expression of three tested transporters was also upregulated in preterm placentas: tryptophan transporter *SLC7A5* ($\log2(FC) = 0.57$, $q < 0.01$) and serotonin transporters *SLC6A4* ($\log2(FC) = 1.07$, $q < 0.0001$) and *SLC22A3* ($\log2(FC) = 1.45$, $q < 0.0001$) (Fig. 1C). The volcano plot (Fig. 1D) further highlighted the genes with the highest fold-changes ($FC > 2$ or $\log2(FC) > 1$): *IDO1*, *SPR*, *ASMT*, *SLC6A4* and *SLC22A3*. In summary, genes involved in placental tryptophan metabolism/transport were mainly more strongly expressed in placentas from preterm births than in term samples.

Table 1. Characteristics of the women included in the study. Presented data are medians with interquartile ranges or percentages

	TERM ($n = 39$)	PTL ($n = 38$)	PPROM ($n = 129$)
Maternal BMI prepregnancy (kg/m^2)	22.20 (20.40–26.30)	22.25 (19.73–25.55)	23.00 (19.95–27.10)
Maternal BMI at admission (kg/m^2)	28.20 (25.20–32.40)	25.05 (23.00–28.58)	26.80 (23.60–32.00)
Newborn weight (kg)	3.47 (3.20–3.82)	1.74 (0.92–2.11)	2.22 (1.85–2.53)
Gestational age at delivery (weeks)	40.00 (39.30–40.60)	31.40 (27.05–33.45)	34.30 (32.80–35.60)
Fetal sex (male %)	61.54	57.89	58.14
Delivery mode (VD:CS)	22:17	31:7	94:35
Primipara (%)	43.59	63.16	54.26
Administration of corticosteroids (%)	0	82.05	83.72
Administration of antibiotics (%)	0	76.62	96.90
Administration of tocolytics (%)	0	52.63	15.50
Induction (%)	0	7.89	17.05
Amniotic fluid IL-6 conc. at admission (ng/ml; measured by *Milenia*)[a]	NA	0.31 (0.050–5.55)	0.16 (0.074–0.42)
Amniotic fluid IL-6 conc. at admission (ng/ml; measured by *Roche*)[a]	NA	2.54 (0.82–13.47)	0.95 (0.40–2.41)
Maternal serum CRP conc. at delivery (mg/l)	NA	10.25 (3.93–40.33)	5.3 (3.00–10.05)
Maternal serum WBC count at delivery ($\times 10^9$ L)	NA	13.93 (11.61–16.26)	13.62 (11.08–16.89)
Apgar score at 5 min <7 (%)	0	13.16	1.55
Apgar score at 10 min <7 (%)	0	5.26	0

[a]Since two methods of measuring amniotic fluid IL-6 were used, the dataset was divided into two subsets: one pertaining to 45 samples (5 PTL and 40 PPROM: 40) and the other pertaining to 111 samples (26 PTL and 85 PPROM) for which the Milenia and Roche techniques were, respectively, used. Amniotic fluid IL-6 concentrations were not determined in 11 samples

Phenotype of preterm delivery (PLT, PPROM) does not affect the placental expression of genes involved in tryptophan metabolism

To identify gene expression signatures within the preterm group, we performed pairwise comparisons of specific groups of preterm placentas, specifically PTL and PPROM versus term placentas. Differences in expression were considered significant if $q < 0.05$ and absolute log2 fold-change >1. The respective volcano plots displayed differences in upregulation of several genes between these two types of placentas. As shown in Figure 2A, two genes were more strongly upregulated in PPROM placentas than in PTL placentas: *SLC6A4* (log2(FC) = 1.09, $q < 0.0001$ in PPROM; log2(FC) = 0.93, $q < 0.0001$ in PTL) and *IDO1* (log2(FC) = 1.49, $q < 0.0001$ in PPROM; log2(FC) = 0.97, $q < 0.05$ in PTL). In addition, as shown in Figure 2B, *TPH2* was more strongly upregulated in PTL placentas (log2(FC) = −0.92, $q < 0.05$ in PPROM; log2(FC) = −1.35, $q < 0.05$ in PTL). Subsequent heatmap analysis of differentially expressed genes with hierarchical clustering was applied to group samples with similar expression levels. The resulting dendrogram (Fig. 2C) identified several clusters of samples, with the term placentas clearly differing from the PTL and PPROM tissues. However, no clear clustering of phenotypes of preterm placentas was observed, suggesting that overall expression of the placental tryptophan metabolic pathway is similarly affected in PTL and PPROM. ANOVA further confirmed the lack of significant differences in the expression of tryptophan pathway genes between PTL and PPROM after FDR correction (Supplementary Material, Table S3). In summary, no significant difference in the expression of genes involved in tryptophan metabolism was observed between PTL and PPROM placentas. Moreover, the differences in gene expression patterns relative to term placentas of the two groups were very similar.

The placental tryptophan pathway gene expression profile of preterm delivery placentas is not affected by MIAC and/or IAI and HCA grades

To identify whether concomitant inflammatory diagnosis associated with preterm deliveries affects placental expression of tryptophan pathway genes, relative gene expression data were subjected to PCA, focusing on possible effects of MIAC and/or IAI and HCA grades (Fig. 3). The first three principal components of this model accounted for high percentages of the overall variance (MIAC and/or IAI, 68.6%; HCA, 69%). About 95% confidence ellipses of all groups overlapped, showing no significant differences in the placental gene expression pattern. ANOVA corroborated the lack of significant difference in placental gene expression between the groups (Supplementary Material, Tables S4 and S5). In summary, no interaction was observed between presence of MIAC and/or IAI and HCA grades and the expression of genes involved in tryptophan pathways.

Unsupervised clustering of preterm delivery placentas shows links between intra-amniotic and maternal inflammation, placental tryptophan pathway gene expression and gestational age at delivery

Unsupervised clustering of 167 placentas based on their gene expression profiles (without *ASMT* and *TPH2*) identified two main clusters (Fig. 4A): one composed of 125 placentas, and the other composed of 42, designated Clusters 1 and 2, respectively. The two clusters had highly differential gene expression. Cluster 1 was associated with high *SLC6A4* ($P < 0.0001$) and *IDO1* ($P < 0.01$) relative expression, while Cluster 2 was linked to upregulation of *KYAT1* ($P < 0.0001$), *HAAO* ($P < 0.0001$), *IDO2* ($P < 0.01$), *KYNU* ($P < 0.0001$), *MAO-A* ($P < 0.0001$), *MAO-B* ($P < 0.0001$), *SLC7A5* ($P < 0.001$), *SLC22A3* ($P < 0.0001$), *SPR* ($P < 0.0001$), *TDO2* ($P < 0.0001$) and *TPH1* ($P < 0.0001$) (Fig. 4B). Stepwise comparison of the two clusters, corrected for fetal sex and maternal BMI at admission, revealed that placentas in Cluster 2 were associated with higher gestational age at delivery (34.3 versus 33.7 weeks, $P = 0.03$) without differences in birth weight (Fig. 4C). Interestingly, Cluster 1 was associated with higher amniotic fluid IL-6 (Roche dataset, $n = 111$) and maternal serum CRP concentrations (Fig. 4D). In contrast, there was no difference in placental *IL6* gene expression between the two clusters.

Characteristics of samples in the two clusters are shown in Figure 5. The fetal sex of placentas in Clusters 1 and 2 was predominantly male and female, respectively ($P = 0.03$) (Fig. 5A). However, despite Cluster 1 including most of the samples, there were no significant differences between clusters in diagnosis (i.e. proportions of PPROM and PTL), HCA grade, parity,

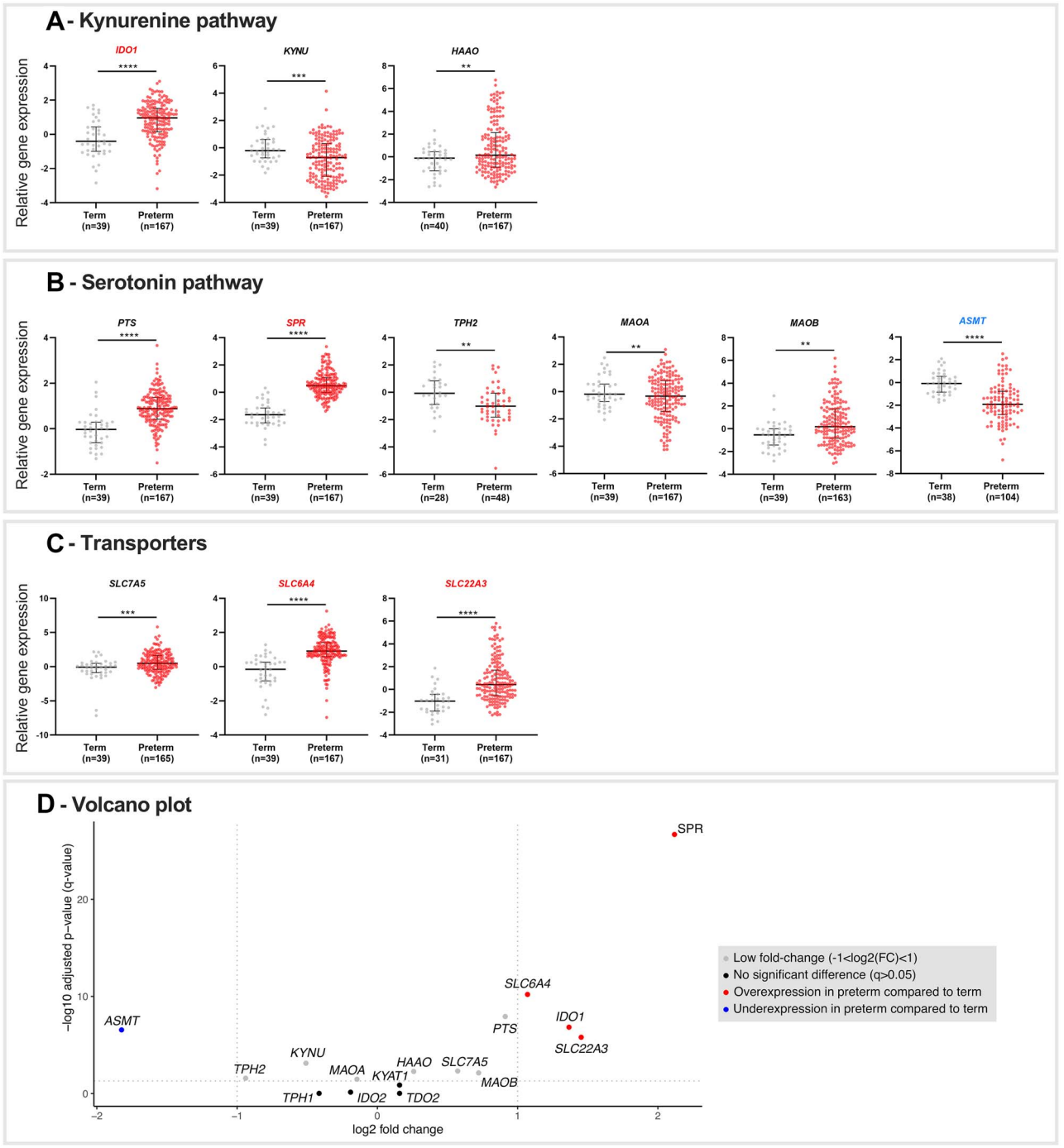

Figure 1. Differentially expressed genes involved in placental tryptophan homeostasis in preterm versus term deliveries. Relative expression of several key enzymes of the kynurenine (**A**) and serotonin pathways (**B**), as well as genes encoding tryptophan and serotonin transporters (**C**), was significantly altered in preterm samples. Data presented in A–C are relative levels of transcripts of indicated genes, normalized with respect to the geometric mean expression of β2-microglobulin (*B2M*) and TATA-binding protein (*TBP*) after log2 transformation, and median values with IQR. Asterisks indicate significance according to type III ANOVA with an FDR correction: **($q \leq 0.01$), ***($q \leq 0.001$), ****($q \leq 0.0001$). (**D**) Volcano plot summarizing the intensity of differential expression between preterm and term placentas. The horizontal axis denotes log2 fold-change, and the vertical axis −log10 transformed corrected *P*-values (*q*-values). Red and blue dots represent significantly differentially expressed genes with absolute log2 fold-change higher than 1.0 and *q*-value of <0.05 (red upregulation and blue downregulation). Gray dots indicate genes with an absolute log2 fold-change less than 1.0 but *q*-value of <0.05, and black dots indicate genes with unaltered expression in preterm births.

delivery mode and pregnancy weight gain (Fig. 5B–F). Moreover, although placentas in Cluster 2 were associated with lower BMI prepregnancy ($P = 0.03$) and at admission ($P = 0.03$) than those in Cluster 1, these differences disappeared when fetal sex was added in the model. There were also no significant differences between antibiotic/tocolytic treatment of the placental donors between Clusters 1 and 2, although more donors of Cluster 1 placentas received corticosteroids than Cluster 2 donors (87.20 versus 73.81%, respectively, $P = 0.04$) and more Cluster 1 donors had IAI (53.3 versus 26.4%, respectively, $P < 0.01$) (Supplementary

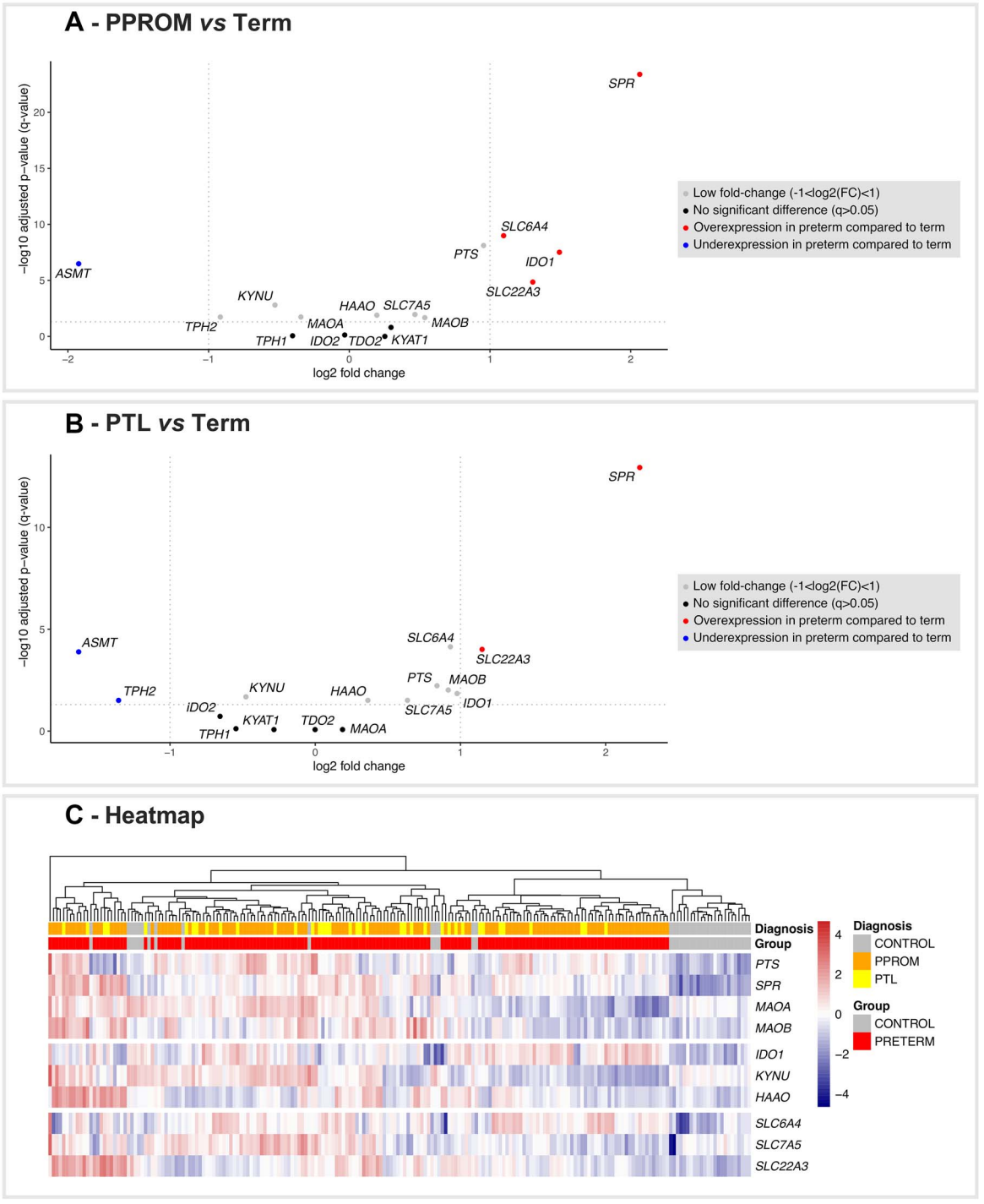

Figure 2. Results of comparative analysis of placental tryptophan pathway gene expression. Volcano plots used to establish the differentially expressed genes between (**A**) PPROM versus term and (**B**) PTL versus term placentas. The horizontal axis denotes the log2 fold-change and the vertical axis represents -log10 transformed corrected P-values (q-values). Red and blue dots indicate significantly differentially expressed genes with absolute log2 fold-change >1.0 and $q < 0.05$ (red upregulation and blue downregulation). Gray dots indicate genes with absolute log2 fold-change <1.0 but $q < 0.05$, and black dots indicate genes with unaltered expression in preterm births. (**C**) Heatmap generated from the log2-transformed expression data for differentially regulated genes, with preterm samples subgrouped into PTL and PPROM samples. The color intensity indicates expression levels (red upregulated and blue downregulated. Between the hierarchical clustering and heatmap, individuals are colored by category. Group separation includes preterm (red) and term (gray) placentas, while diagnosis highlights term (gray), PPROM (orange) and PTL (yellow) placentas.

Material, Table S6). In summary, unsupervised clustering of PCA-separated samples distinguished two clusters that differed in placental gene expression among the preterm samples. Placentas in Cluster 2 were associated with higher gestational age at delivery, but lower amniotic fluid IL-6 and maternal serum CRP concentration.

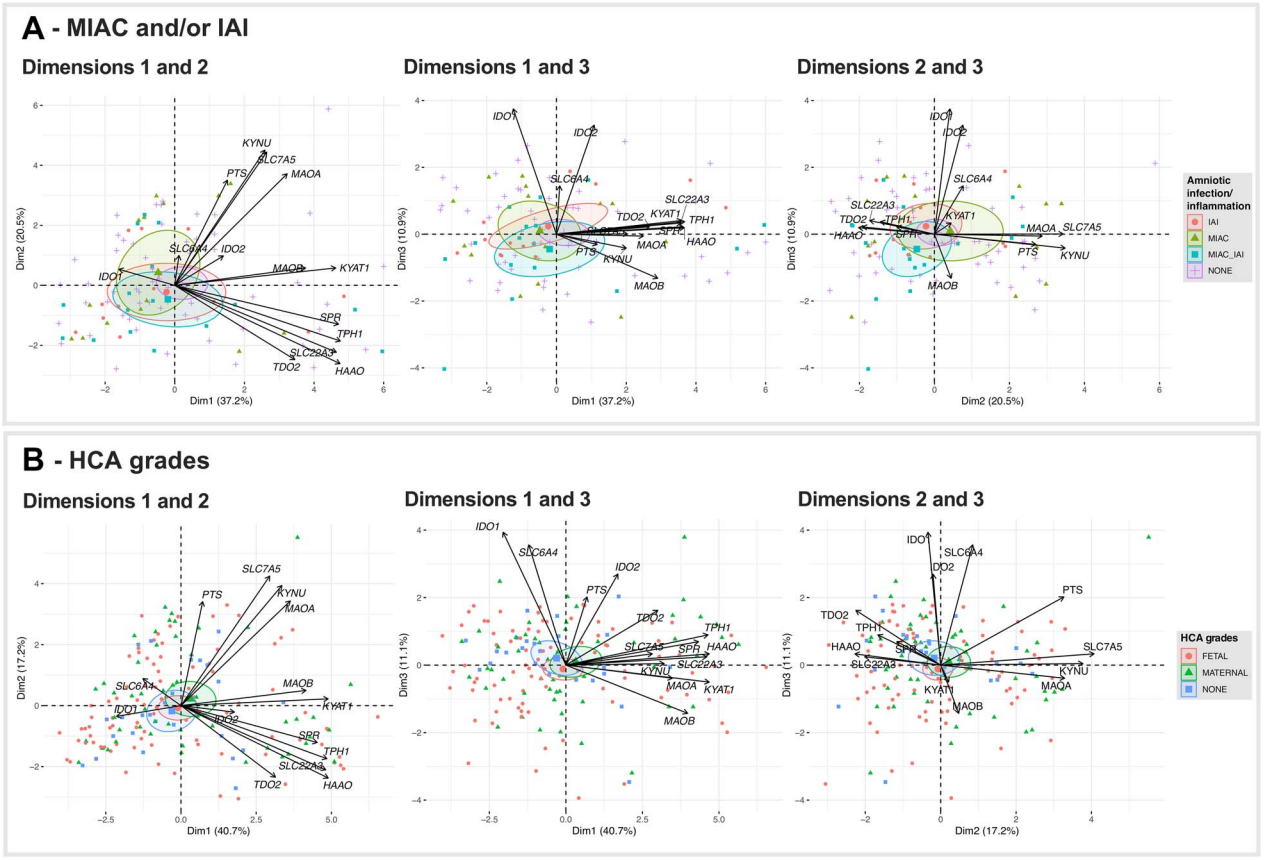

Figure 3. Principal component analysis (PCA) biplots visualizing placental tryptophan pathway gene expression in preterm delivery placentas. (**A**) Positions of individual and subgroups of placentas in the first, second and third dimensions (accounting for 37.2, 20.5 and 10.9% of explained variance, respectively) in biplots [MIAC (colonization), MIAC and IAI (intra-amniotic infection), IAI (sterile IAI), and none (neither MIAC nor IAI)] and vectors of expression of indicated genes (black arrows). (**B**) Positions of placentas associated with indicated HCA grades [fetal (fetal inflammatory response), maternal (maternal inflammatory response) or none (absence of HCA)] in the first, second and third dimensions (accounting for 40.7, 17.2 and 11.1% of explained variance, respectively) in biplots and vectors of expression of indicated genes variables (black arrows). A 95% confidence ellipse was drawn around the barycenter for each group. The gene expression data were log2 transformed prior to analysis.

Relationships between intra-amniotic and maternal inflammation markers, placental tryptophan metabolism and gestational age at delivery

As Cluster 2 was associated with higher gestational age at delivery than Cluster 1, we applied the Pearson correlation test to identify genes whose expression correlated with gestational age in the preterm birth samples. Of the genes tested, relative expression of *IDO2* ($r = 0.33$, $P < 0.0001$), *KYAT1* ($r = 0.20$, $P = 0.01$) and *TPH1* ($r = 0.17$, $P = 0.02$) was moderately correlated with gestational age at delivery (Fig. 6A). Expression of one of these genes, *KYAT1*, also correlated with amniotic fluid IL-6 (Roche dataset; $n = 111$, $r = -0.23$, $P = 0.01$) and maternal serum CRP (whole dataset; $r = -0.21$, $P < 0.01$) concentrations, while concentrations of both inflammatory markers correlated with gestational age at delivery ($r = -0.26$, $P < 0.001$ and $r = -0.39$, $P < 0.0001$, respectively) (Fig. 6B and C). Intercorrelations between gestational age at delivery, inflammatory marker concentrations and gene expression data presented in Figure 6D confirm that both IL-6 amniotic fluid and maternal serum CRP concentrations were negatively correlated with gestational age at delivery, and *KYAT1* expression was most strongly correlated with both maternal CRP concentration and gestational age at delivery.

To complete the investigation, we performed a mediation analysis, which confirmed that maternal serum CRP concentration, and to a lesser extent, amniotic fluid IL-6 concentration (Roche dataset, Supplementary Material, Table S6), significantly mediated the relationship between placental gene expression and gestational age at delivery (Fig. 6E). Linear regression models were adjusted for the delivery mode and pregnancy weight gain, which were consistently highly significant ($P < 0.0001$ for both covariates). The mediation effect of amniotic fluid IL-6 concentration was complete for both adjusted and non-adjusted models. In contrast, the mediation effect of maternal serum CRP concentration was complete for the unadjusted model, but the direct effect of *KYAT1*'s relative expression on gestational age at delivery was no longer statistically significant when adjusted for covariates.

Globally, *KYAT1* gene expression and concentrations of inflammatory markers were directly and significantly linked to gestational age at delivery, and significantly associated with each other. The mediation effect (ab) was consistently significant, confirming that concentrations of inflammatory markers significantly mediated the effect of gene expression on gestational age at delivery. Complete results of the mediation analysis are displayed in Supplementary Material, Table S7.

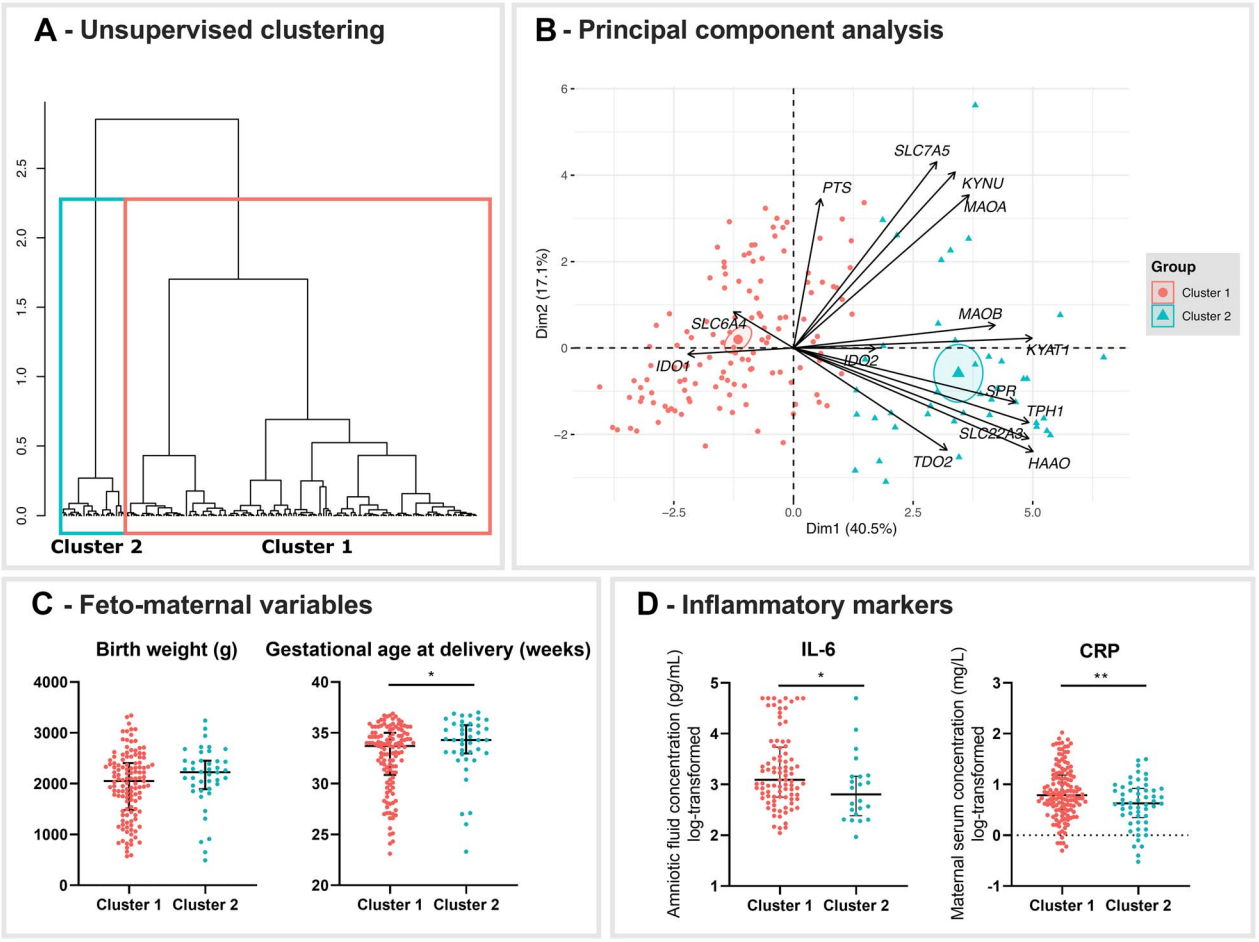

Figure 4. Unsupervised clustering of placentas from preterm births based on expression of genes involved in tryptophan metabolism. (**A**) Analysis of 167 placentas identified two main clusters: Cluster 1 represented in red ($n = 125$) and Cluster 2 in blue ($n = 42$). (**B**) Cluster 1 was positively linked with high relative expression of *IDO1* and *SLC6A4* gene expression, while Cluster 2 was positively associated with high relative expression of *KYAT1*, *HAAO*, *IDO2*, *KYNU*, *MAO-A*, *MAO-B*, *SLC7A5*, *SLC22A3*, *SPR*, *TDO2* and *TPH1*. (**C**) Cluster 2 was associated with higher gestational age at delivery, but lower concentrations of inflammatory markers, specifically amniotic fluid IL-6 (Roche dataset, $n = 111$), and maternal serum CRP (**D**). The significance of differences between the clusters was assessed using the chi-square test (B) or type III ANOVA (C and D) with fetal sex and maternal BMI at admission treated as covariates. Gene expression data were log2 transformed, while amniotic fluid IL-6 and maternal serum CRP concentrations were log transformed before analysis. *($P \leq 0.05$), **($P \leq 0.01$).

In summary, amniotic fluid IL-6 concentrations at admission and maternal serum CRP levels at delivery were negatively correlated with gestational age at delivery. Expression of one gene (*KYAT1*) also correlated with gestational age at delivery and both intra-amniotic and maternal inflammatory marker concentrations. Mediation analysis showed that concentrations of inflammatory markers mostly mediated the effect of placental gene expression on gestational age at delivery, but this mediation was weakened by the delivery mode and pregnancy weight gain.

Correlations between placental *IL6* gene expression and relative expression of genes involved in the tryptophan pathway and metabolism were also analyzed (Fig. 7). We found that placental *IL6* gene expression was weakly to moderately correlated with the relative expression of *HAAO* ($r = 0.20$, $P = 0.01$), *IDO1* ($r = 0.24$, $P < 0.01$), *IDO2* ($r = 0.38$, $P < 0.0001$), *SLC22A3* ($r = 0.16$, $P = 0.04$), *SPR* ($r = 0.20$, $P = 0.01$), *TDO2* ($r = 0.25$, $P < 0.01$), *TPH1* ($r = 0.20$, $P = 0.01$), *KYNU* ($r = -0.18$, $P = 0.02$) and *MAO-A* ($r = -0.18$, $P = 0.02$), suggesting a relationship between *IL6* and placental tryptophan pathway. We also evaluated the relation between amniotic fluid IL-6 concentration and placental *IL6* relative expression in the subgroup of placentas from pregnancies in which the time between admission and delivery was <72 h but detected no significant correlation (data not shown).

Discussion

We examined transcriptional profiles and inflammatory markers in placentas from healthy and preterm birth pregnancies. Using robust multivariate statistical methods, we detected clear systematic differences in their expression of tryptophan pathway genes (mostly upregulated in preterm pregnancies). Moreover, we found that this effect is statistically associated with the intra-amniotic and maternal inflammatory markers. In addition, unsupervised clustering of samples from the preterm birth cohort identified two molecular placental subtypes.

The dominant subtype was characterized by a lower gestational age at delivery, higher amniotic fluid IL-6 and maternal serum CRP concentrations, and differential placental tryptophan pathway expression (Fig. 8). Such segregation of placentas associated with preterm delivery, based on levels of inflammatory and chemokine markers, has also been previously reported,

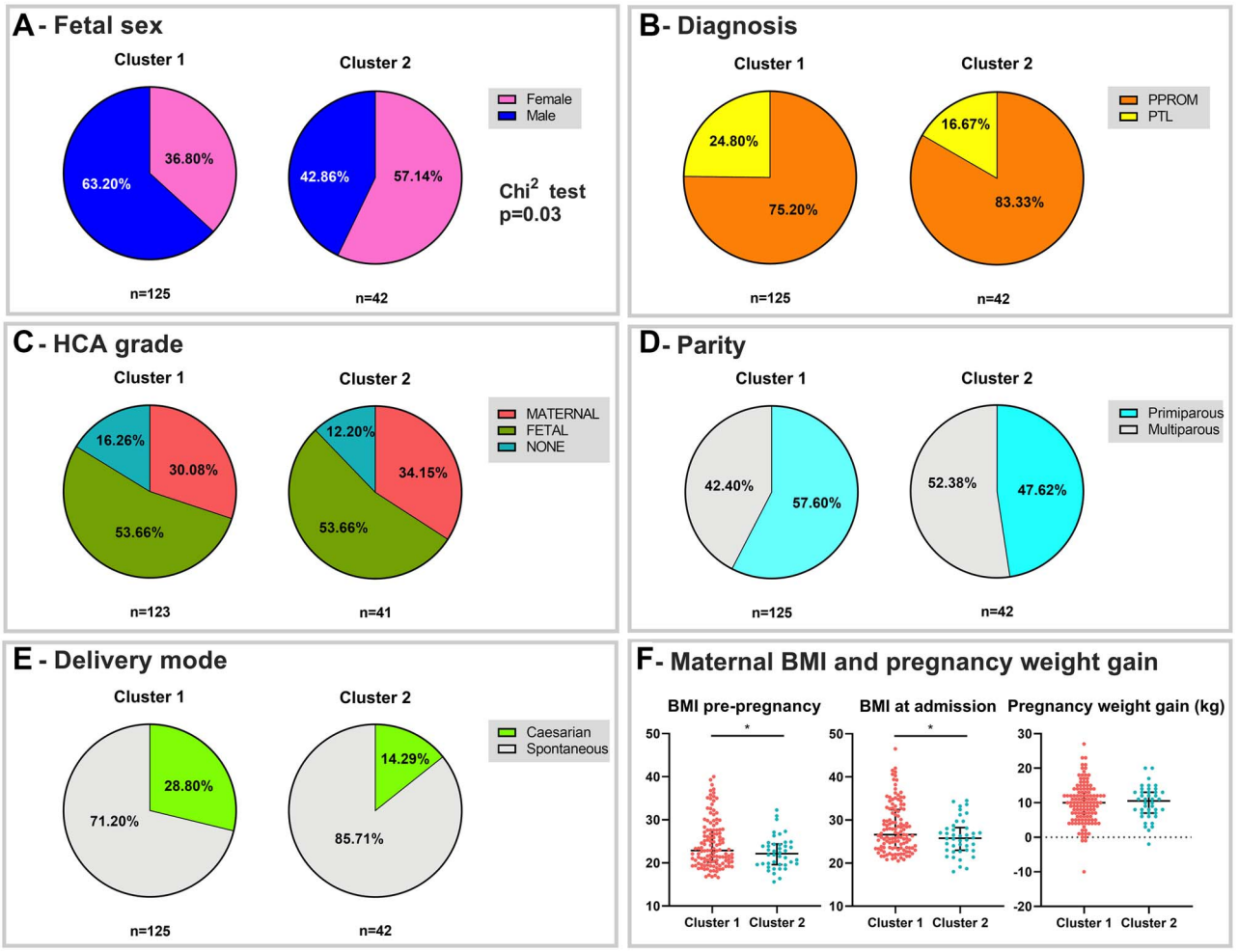

Figure 5. Comparison of characteristics of samples in Clusters 1 and 2. Distributions of fetal sex (**A**), diagnosis (**B**), presence of HCA (**C**), parity (**D**), delivery mode (**E**), maternal BMI (prepregnancy and at admission) and pregnancy weight gain (**F**). *($P \leq 0.05$).

suggesting that although PTL and PPROM have distinct clinical presentations they may share common inflammatory etiologies (27). Notably, concentrations of amniotic fluid IL-6 and maternal CRP were negatively correlated with gestational age at delivery, suggesting that inflammatory processes are involved in preterm delivery. Accordingly, prenatal inflammation often results in preterm delivery, which is, regardless of infection, associated with elevated maternal serum and amniotic fluid IL-6 concentrations (28,29). Previous research has shown that increased maternal CRP levels are significantly associated with schizophrenia (30) and autism (31) in offspring. Similarly, elevated maternal IL-6 concentrations, especially maternal IL-6 concentrations in the third trimester, are predictive of impaired working memory outcome (32). Moreover, exogenous administration of IL-6 to pregnant mice induces behavioral changes in the offspring, which are prevented by IL-6 knockout or anti–IL-6 antibodies (33). Thus, CRP and IL-6 are apparently crucial immunological mediators linking maternal immune activation with poor neurobehavioral development. However, the mechanisms involved in fetal neuroprogramming remain to be elucidated.

Elevated maternal IL-6 has been shown to increase placental IL-6 content (34,35); however, in this study, we did not observe any correlation between placental *IL6* gene expression and IL-6 concentrations in the amniotic fluid. Nonetheless, we show that placental *IL6* expression is correlated to expression of several genes involved in serotonin and kynurenine pathways of tryptophan metabolism. Indeed, maternal IL-6 has been shown to enter the placenta (36), where it activates the placental JAK/STAT3 pathway and affects expression of acute-phase genes (35). Further research is necessary to understand the mechanisms involved and their physiological relevance. On the other hand, maternal CRP is not transported across the placenta to the fetus (37), possibly due to its deposition in the placenta (38), where it may interfere with placental functions or act as a proxy for IL-6 (30). Collectively, our results and previous findings indicate that in pregnancies associated with preterm birth IL-6, and potentially CRP, act in concert with several essential placental genes, including those involved in tryptophan metabolism/transport, thereby perturbing normal placental functions.

The major route of tryptophan catabolism is via the kynurenine pathway, generating kynurenines, which have anti-inflammatory and immunosuppressive actions (12). In our study, we found that *KYAT1* expression was negatively correlated with intra-amniotic/maternal inflammatory markers. We thus speculate that the kynurenine pathway may be altered in pregnancies associated with preterm birth and involved in placental protection against inflammation. However, further

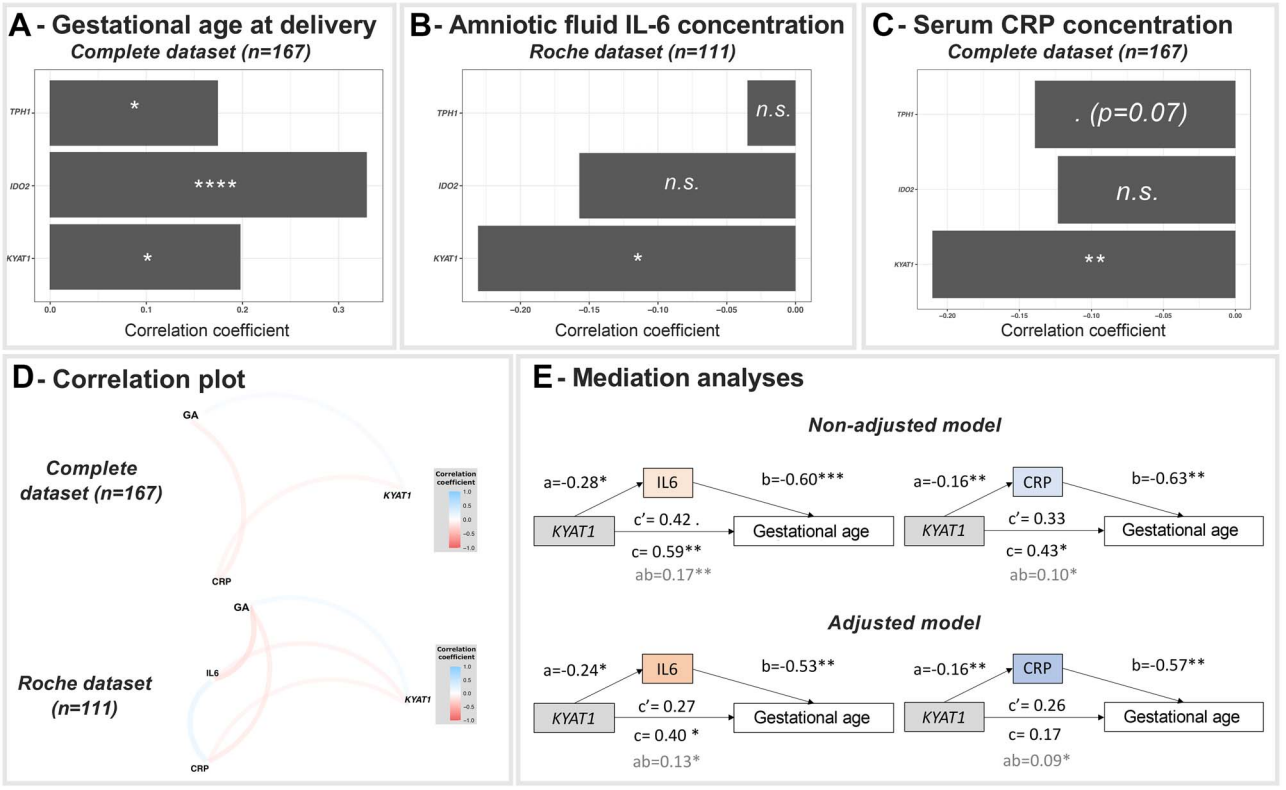

Figure 6. Relationships between placental gene expression, gestational age at delivery and inflammatory markers in preterm samples. Significant correlations ($P < 0.05$) between relative gene expression and gestational age at delivery (**A**), amniotic fluid IL-6 concentration (Roche dataset, $n = 111$) (**B**), and serum CRP concentration (whole dataset, $n = 167$) (**C**) are shown. (**D**) Correlation plot (Pearson correlation coefficient, $r > 0.19$) indicating the dependence between gene expression, gestational age at delivery (GA) and concentration of inflammatory markers. The intensity of correlations varies between red (negative) and blue (positive). The closer the variables, the stronger the correlation. (**E**) Results of mediation analysis: numbers displayed are beta-coefficients from the linear model, and those marked with asterisks significantly differ from zero. a is the direct effect between relative gene expression and inflammatory marker concentration. b is the direct effect between inflammatory marker concentration and gestational age at delivery. c′ is the direct effect between relative gene expression and gestational age at delivery after adjusting for inflammatory marker concentration. c is the total effect, i.e. direct effect of relative gene expression on gestational age at delivery. ab is the mediation effect, i.e. effect of gene expression on gestational age at delivery through the concentration of inflammatory markers. If c′ remains significant, the mediation is partial, but if insignificant, the mediation is complete. Indicated significance was obtained by the Pearson test (a, b and c) or from a linear model (e). For mediation analysis, delivery mode and pregnancy weight gain were treated as covariates. Gene expression data were log2 transformed, and amniotic fluid IL-6 and maternal serum CRP concentrations were log transformed. *($P \leq 0.05$), **($P \leq 0.01$), ***($P \leq 0.001$), ****($P \leq 0.0001$).

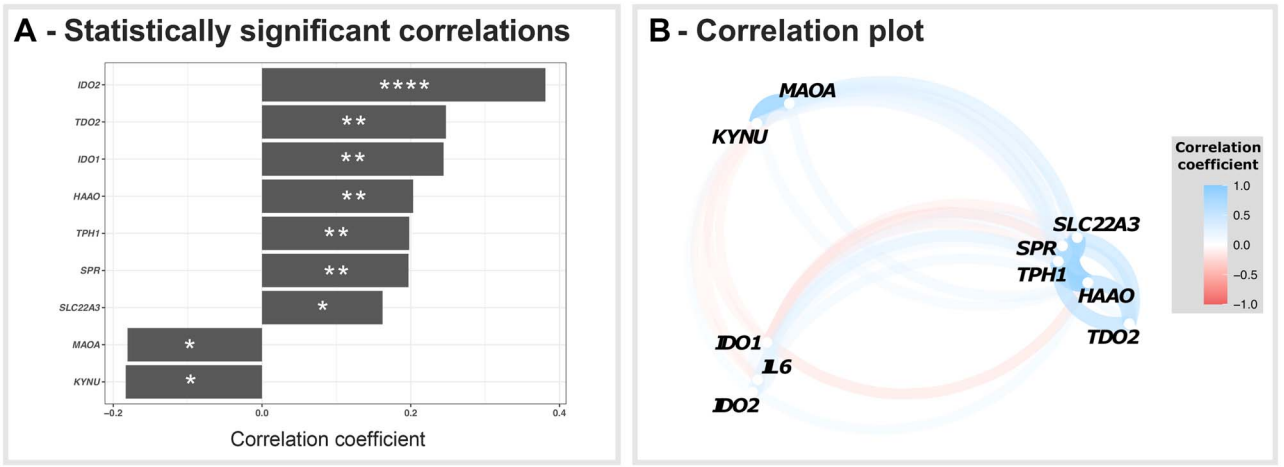

Figure 7. Relationship between placental *IL6* gene expression and relative expression of genes involved in placental tryptophan homeostasis. (**A**) Significant correlations ($r > 0.15$, $P < 0.05$; according to the Pearson test) were detected for several genes involved in metabolism/transport of tryptophan. (**B**) Correlation plot depicting the intensity of relationships varying between red (negative) and blue (positive); the closer the variables, the stronger the correlation. *($P \leq 0.05$), **($P \leq 0.01$), ****($P \leq 0.0001$).

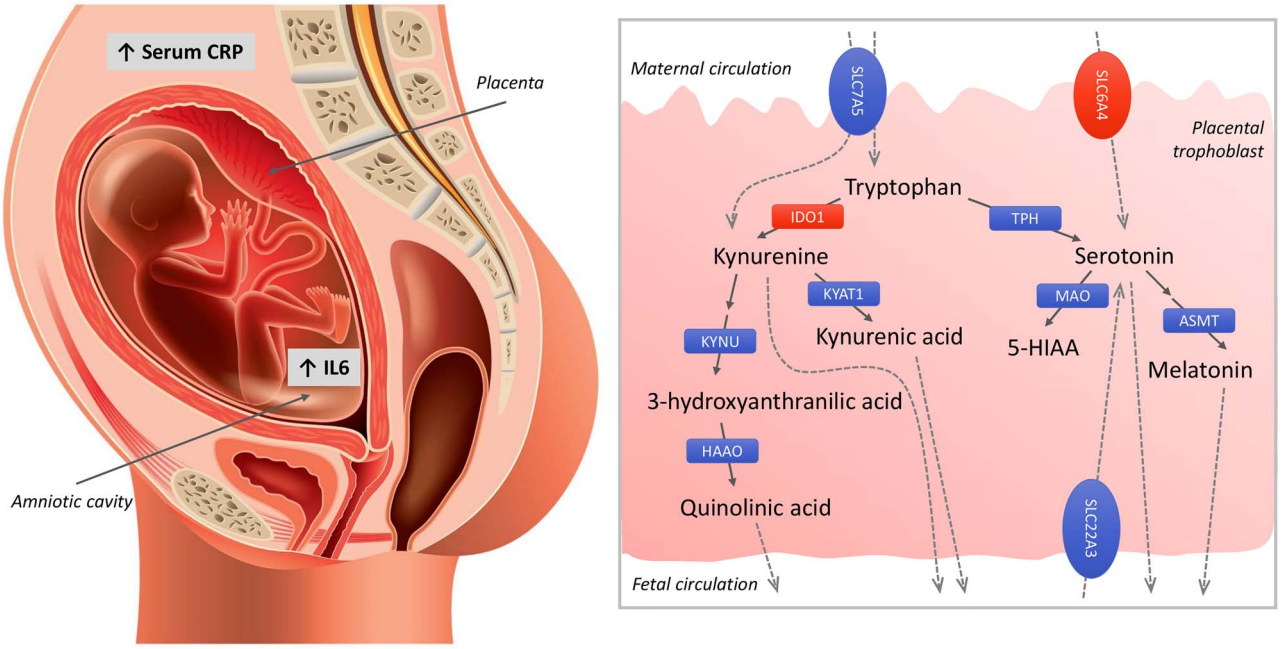

Figure 8. Graphical representation of the dominant molecular placental subtype associated with preterm delivery, identified by unsupervised clustering analysis. This cluster is characterized by a highly inflammatory environment with upregulated amniotic fluid IL-6 and maternal serum CRP levels. Compared with the low inflammation subtype, this high inflammation profile is associated with differentially expressed placental expression of tryptophan metabolism pathways (red upregulation, blue downregulation).

research is needed to confirm whether kynurenine metabolites participate in buffering the inflammatory response (39). It would also be interesting to compare the neurodevelopment of children with preterm births linked to Clusters 1 and 2 to assess potential protective effects of the differences in concentrations of inflammatory markers, gestational age at delivery and expression of placental genes involved in tryptophan metabolism.

In placentas associated with preterm deliveries, we detected significant upregulation of *SLC7A5*, encoding a transporter of large, neutral amino acids including tryptophan, compared with placentas associated with term births, suggesting that they may obtain more maternal tryptophan. Previous research has also shown that *in utero* inflammation in mice significantly increases tryptophan levels in the amniotic fluid and fetal brain (40) and maternal inflammation in midpregnancy leads to a transient increase in placental tryptophan content (25). Upregulation of *IDO* and increased rates of tryptophan metabolism via the kynurenine pathway may directly or indirectly lead to exposure of the developing fetal brain to neuroactive kynurenine metabolites. Indirectly, placental kynurenine metabolism ultimately leads to the generation of neuroactive QUIN and kynurenic acid (KYNA) (12). Although scarce, reports have also associated upregulation of QUIN-producing enzymes with inflammatory cytokines (14). Accordingly, increased levels of QUIN in umbilical venous blood have been detected in PPROM pregnancies compared with pregnancies leading to healthy term deliveries (15). Moreover, prenatal inflammation has been shown to increase KYNA levels in the fetal brain (40). We observed a negative relationship between *KYAT1* expression and prenatal inflammation, suggesting that it may be a placental-independent effect or an alteration affecting the downstream protein production and/or enzyme activity. A previous report that KYNA output is not affected in pregnancies with intrauterine infection provides further support for our findings (15). Thus, it is likely that placental *IDO* induction can directly increase kynurenine output to the fetus via *SLC7A5*, which is also capable of transporting kynurenine (41). This may result in increased fetal brain kynurenine concentrations and local production of KYNA. However, this hypothesis remains to be confirmed.

Regarding the serotonin pathway, we have previously shown that at term the placental role in serotonin homeostasis is mainly maintained by the coordinated activity of serotonin uptake transporters (SERT/SLC6A4 and OCT3/SLC22A3) and serotonin-degrading enzyme (MAO-A) (42). Here we observed that expression of both *SLC6A4* and *SLC22A3* transporters is upregulated in placentas associated with preterm birth compared with those associated with term births, in accordance with previous findings of cytokine-upregulated SERT expression (43). The alterations in expression of transport systems (but not the metabolizing enzyme) could lead to serotonin accumulation in the placenta. As a potent vasoconstrictor, serotonin could affect placental vascularization. This hypothesis is consistent with reported associations between placental vascular abnormalities and preterm birth (44), and effects of cytokines on expression of vascularization factors (45). Moreover, apart from its direct vasoconstrictive effect, serotonin can also indirectly affect expression of vascularization factors through hypoxia (46). Unfortunately, to our knowledge, no previous study has measured maternal/umbilical artery or placental serotonin concentrations in preterm and term pregnancies. We can only speculate from the results presented here that serotonin concentrations in the fetoplacental unit might be higher in pregnancies associated with preterm deliveries. Whether *MAO-B* upregulation can contribute to serotonin degradation is yet to be determined. MAO-B expression is reportedly expressed consistently (at low levels) in mitochondrial preparations of human placenta (47,48); thus, its activity cannot be excluded.

Taken together, our findings show that preterm birth is associated with significant changes in placental tryptophan metabolism that may be involved in fetal programming of neurodevelopmental disorders. Importantly, we show that in this respect PTL and PPROM placentas do not significantly differ and we did not identify substantial differences based on MIAC and/or IAI and grades of HCA.

A key strength of this study is the inclusion of placental samples from a large and well-characterized cohort of women who had preterm deliveries, with thoroughly defined specific phenotypes, allowing application of multiple statistical methods to interpret the findings. As with other studies on preterm birth, this study is limited by the lack of normal age-matched controls making it difficult to distinguish gestational age differences from those associated with the pathology. Likewise, since none of the healthy term deliveries were administered corticosteroids, this effect could not be controlled in our statistical analysis. Thus, further research is required to determine a potential causal relationship between corticosteroid administration and differential placental tryptophan pathway expression in preterm delivery. Lastly, while we provide insights into transcriptional mechanisms contributing to alterations in placental function and perhaps developmental processes in the fetal brain, further studies are required to examine the functional extent of these changes.

Materials and Methods

Placenta sample collection

Samples were collected at the Department of Obstetrics and Gynecology, University Hospital in Hradec Kralove, Czech Republic. Human term, PTL and PPROM placentas were obtained immediately after delivery, upon obtaining the women's written informed consent. The study was performed in accordance to the ethical standards laid down in the 1964 Declaration of Helsinki and was approved by the Research Ethics Committee of the University Hospital in Hradec Kralove, Czech Republic (Approval No. 201006 S15P). Samples were collected between August 2015 and June 2020. Samples from healthy term pregnancies were snap-frozen in liquid nitrogen and stored at −80°C until analysis. The samples from PTL and PPROM pregnancies were stored in RNAlater™ (Invitrogen, Carlsbad, CA) at −80°C until analysis. Women with preeclampsia, diabetes mellitus, gestational diabetes mellitus, gestational hypertension and complications such as structural malformations or chromosomal abnormalities of the fetus, fetal growth restriction, vaginal bleeding and/or signs of fetal hypoxia were excluded from the study.

Clinical definitions and diagnostic pathology

Gestational age was established by first-trimester fetal biometry. PTL was diagnosed as the presence of regular uterine contractions (at least two every 10 min), along with cervical length, measured using transvaginal ultrasound, shorter than 15 mm or within the 15–30 mm range with a positive PartoSure test (Parsagen Diagnostics Inc., Boston, MA) (49). PPROM was diagnosed by examining the women, using a sterile speculum, for pooling of amniotic fluid in the posterior fornix of the vagina. If there was clinical uncertainty in diagnosing PPROM, amniotic fluid leakage was confirmed by the presence of insulin-like growth factor-binding proteins using an Actim PROM test kit (Medix Biochemica, Kauniainen, Finland) in the vaginal fluid.

Women with PTL received a course of corticosteroids (betamethasone) and tocolytic therapy with either intravenous atosiban (for gestational age ≤28 weeks) or nifedipine, administered orally, for 48 h. Patients with proven intra-amniotic inflammation received treatment with intravenous clarithromycin for 7 days, unless delivery occurred earlier. Antibiotic treatment was modified if microbial invasion of the amniotic cavity occurred. Women with PTL who were positive for group B Streptococcus (GBS), determined from vaginal–rectal swabs, or had unknown GBS status, received intravenous benzylpenicillin (clindamycin, in case of penicillin allergy) during an active labor (50).

Women with PPROM were treated with antibiotics. Those with intra-amniotic inflammation received first-line treatment with intravenous clarithromycin for 7 days. Unless delivery occurred earlier, the antibiotic treatment was modified if microbial invasion of the amniotic cavity occurred; the women without intra-amniotic inflammation received benzylpenicillin (or clindamycin, for women allergic to penicillin). Women with PPROM with gestational age <35 weeks received corticosteroids (betamethasone) to accelerate fetal lung maturation and reduce neonatal mortality and morbidity. Women with PPROM were managed expectantly, except those with intra-amniotic infection and gestational age >28 weeks, for whom labor was induced or an elective cesarean section was performed within 72 h of admission (50).

Ultrasound-guided transabdominal amniocentesis was performed on admission to all women with PTL and PPROM, prior to administration of corticosteroids, antibiotics or tocolytics, to investigate the intra-amniotic environment. Amniotic fluid was used for interleukin-6 (IL-6) assessment and determination of MIAC, as previously described (51). At the time of delivery, maternal blood samples were obtained via venipuncture of the cubital vein and sent to the laboratory to determine their white blood cell (WBC) count and levels of C-reactive protein (CRP) immediately following sampling. After delivery, tissue-block sections of placenta, umbilical cord and fetal membranes were placed in paraffin and stained with hematoxylin and eosin for standard histological examination. This examination was performed by a single perinatal pathologist who was blinded to the clinical status of the samples.

Amniotic fluid IL-6 levels were assessed, in the samples obtained from August 2015 to November 2018, using a Milenia QuickLine IL-6 lateral flow immunoassay kit and Milenia POC-Scan Reader (Milenia Biotec, GmbH, Giessen, Germany) (51). Samples obtained between December 2018 and June 2020 were evaluated using an automated electrochemiluminescence immunoassay method with a Cobas e602 immunoanalyzer, which is part of the Cobas 8000 platform (Roche Diagnostics, Basel, Switzerland).

IAI was defined as a concentration of IL-6 in amniotic fluid ≥745 pg/ml, measured using a lateral flow immunoassay point-of-care test (52,53), or ≥3000 pg/ml measured using an automated electrochemiluminescence immunoassay method (54). MIAC was determined based on a positive PCR analysis of *Ureaplasma* species, *Mycoplasma hominis, Chlamydia trachomatis* or a combination of these species, or positivity for the 16S rRNA gene, aerobic/anaerobic cultivation of the amniotic fluid or a combination of these parameters. Based on the MIAC and/or IAI test results, women were divided into four groups: intra-amniotic infection (both MIAC and IAI), sterile IAI (IAI alone), colonization (MIAC alone) and negative (neither MIAC nor IAI). Finally, the degree of neutrophil infiltration was evaluated as previously described (55) and according to well-established criteria (56). Diagnosis of acute histological chorioamnionitis

(HCA) was based on presence of histological grades of chorion–decidua 3–4, chorionic plate 3–4, umbilical cord 1–4 and/or amnion 1–4 (56). The following HCA grades were used to describe the intensity of placental inflammatory response: maternal inflammatory response (presence of histological grades of chorion–decidua 3–4 and/or chorionic plate 3 and/or amnion 1–4) and fetal inflammatory response (presence of histological grades of chorionic plate 4 and/or umbilical cord 1–4).

RNA isolation and reverse transcription

Total RNA was isolated from weighed tissue samples using Tri Reagent (Molecular Research Center, Cincinnati, USA) following the manufacturer's instructions. Concentrations of RNA were determined from measurements of absorbance (A) at 260 nm, and its purity was evaluated by determining A260/280 and A260/230 ratios using a NanoDrop™ 1000 Spectrophotometer (Thermo Fisher Scientific, Waltham, MA, USA). Samples were not included in subsequent analysis if their A_{260}/A_{280} ratio < 1.60 and A_{260}/A_{230} ratio < 1.80.

RNA integrity was confirmed by electrophoresis on a 1.5% agarose gel. Portions (1 µg) of total RNA were reversely transcribed to cDNA in reaction mixtures with a total volume of 20 µl using an iScript cDNA Synthesis Kit (Bio-Rad, Hercules, CA, USA) and a Bio-Rad T100™ Thermal Cycler (Hercules, CA, USA) with the following conditions: 5 min at 25°C, 20 min at 46°C and 1 min at 95°C. Obtained cDNA was stored at −20°C until use.

Quantitative PCR analysis

Samples of the collected placentas were subjected to quantitative PCR (qPCR) gene expression analysis using a CFX384 Touch™ Real-Time PCR Detection System (Bio-Rad, Hercules, CA, USA). cDNA (12.5 ng/µl) was amplified in a 384-well plate, with total reaction volumes of 5 µl per well, using SsoAdvanced™ Universal SYBR® Green Supermix (Bio-Rad, Hercules, CA, USA) and predesigned intron-spanning PrimePCR™ assays (listed in Supplementary Material, Table S1). Each sample was amplified in triplicate, with the following conditions: 2 min at 95°C followed by 40 cycles of 5 s at 95°C and 30 s at 60°C, then a final 5 s at 95°C. For melt curve analysis, the temperature was raised from 65 to 95°C, with 0.5°C increments at 5 s/step.

qPCR analysis was performed with CFX Maestro™ Software (Bio-Rad, Hercules, CA, USA). Before the quantitative analysis, we assessed the stability of candidate reference genes' expression in our samples using the RefFinder web-based analysis tool (57), which implements four algorithms: Delta Ct (58), BestKeeper (59), geNorm (60) and NormFinder (61). Commonly used reference genes tested included genes encoding β2-microglobulin (*B2M*), ubiquitin (*UBQ*), glyceraldehyde 3-phosphate dehydrogenase (*GAPDH*), tyrosine 3-monooxygenase/tryptophan 5-monooxygenase activation protein zeta (*YWHAZ*), 18 s ribosomal RNA (*18 s rRNA*) and TATA-binding protein (*TBP*). Finally, target gene expression was normalized against the mean quantification cycle of *B2M* and *TBP* using the Bio-Rad CFX Maestro 1.1 software.

Minimum information for publication of real-time quantitative PCR experiments (MIQE) guidelines (62,63) were followed during all steps in efforts to ensure accuracy, correct interpretation and repeatability of the results obtained from this study. The MIQE checklist is provided in Supplementary Material, Table S2.

Statistical analysis

Differential gene expression analysis. Relative gene expression results obtained using Bio-Rad CFX Maestro 1.1 software were log2 transformed before analysis. Statistical analyses and graphical representation were performed using Rstudio (version 1.3.1093, R software version 4.0.3) and GraphPad Prism (version 8.2.1). Results were considered statistically significant when $P < 0.05$.

Preterm versus term and PPROM versus PTL placentas. Differences in relative gene expression between preterm and healthy term placentas were explored by type III ANOVA, using the car package (64). Covariates, such as fetal sex, delivery mode (vaginal delivery versus cesarean section) and maternal pregnancy weight gain, were considered in the model when statistically significant. To account for multiple analyses, *P*-values were adjusted using false discovery rate (FDR) correction and are presented as *q*-values. Graphical representation was performed using GraphPad Prism; results are shown as median and interquartile ranges (IQR).

The same methods were applied to analyze the differences between PPROM versus term and PTL versus term placentas. Corrected *P* values were subsequently used to generate volcano plots using the ggplot2 package (65) after calculating log2 fold-changes (log2(FC)) and -log10 transformation of the *q*-values.

Finally, a heatmap of the differentially expressed genes was generated using the pheatmap package (66). Within-gene and between-individual (row) data scaling was applied. Hierarchical clustering (Euclidian distances) was applied to individuals only. Missing data were imputed using principal component analysis (PCA) with the missMDA package (67). *ASMT* and *TPH2* expression was not included in these analyses as it was not detected in a large number of samples by qPCR analysis, so it could not be imputed.

Principal component analysis: preterm placentas. PCA was used to explore and interpret patterns in the multivariate interrelated datasets by reducing the dimensionality of the high-dimensional data to a low-dimensional format while preserving the relevant information. Samples were grouped based on the grades of HCA. In addition, data regarding placentas of the subset of women with PPROM and a period <72 h between amniocentesis and delivery were used to create a PCA plot of patterns associated with MIAC and/or IAI.

Log2-transformed relative gene expression data were analyzed, after scaling, using the PCA function in the FactoMineR package (68). Positions of individuals and variables along the first three principal components were graphically displayed in biplots using the fviz_pca_biplot function of the factoextra package (69). Then, a 95% confidence ellipse was drawn around the barycenter of each group.

Unsupervised clustering: preterm placentas. PCA was applied to the whole dataset of preterm placentas to reduce its dimensionality. Unsupervised clustering was then applied, using the hcpc function of the FactoMineR package (68), in the resulting model's first five dimensions (accounting for 81% of the total variance). Differences in clinical maternal and fetal variables (gestational age at delivery, birth weight, maternal prepregnancy BMI and BMI at admission, and pregnancy weight gain) and concentrations of inflammatory markers (amniotic fluid IL-6, log-transformed; maternal serum CRP at delivery, log-transformed; and maternal white blood cells count at delivery) between clusters were

explored using type III ANOVA with the car package. For amniotic fluid IL-6 concentration, the dataset was divided according to the measurement method (Milenia or Roche system). Graphical representation was performed using GraphPad Prism; results are shown as median and interquartile ranges (IQR). The significance of differences in proportions of individuals in each pregnancy category such as fetal sex, diagnosis (PTL/P-PROM), parity, delivery mode (vaginal delivery versus cesarean section), antibiotics, tocolytics and corticosteroids treatment was assessed by chi-squared tests implemented in GraphPad Prism.

Correlations between gene expression, inflammatory markers and gestational age at delivery: mediation analysis. Correlation analyses were performed to establish associations between placental tryptophan pathway, gestational age at delivery and concentrations of intra-amniotic and maternal inflammatory markers. First, Pearson correlations between gene expression levels and gestational age at delivery were calculated using the rcorr function of the Hmisc package (70). Correlations between genes whose expression was significantly associated with gestational age at delivery and concentrations of the intra-amniotic and maternal inflammatory markers were then examined, followed by correlations between concentrations of intra-amniotic and maternal inflammatory markers and gestational age at delivery. Significant correlations were represented in focus graphs or correlation plots displaying the interrelations between all the variables tested using the correlate and network plot functions of the corrr (71) and ggplot2 (65) packages.

For mediation analysis, direct effects of genes' expression ('treatment') on concentrations of intra-amniotic and maternal inflammatory markers (mediators) and these mediators on gestational age at delivery ('the outcome') were estimated using regression analyses. Bootstrap permutations ($P = 1000$) were used to estimate the total effect (direct effect of treatment on the outcome), the direct effect of treatment on outcome after adjusting for the mediators and the mediation effect using the function mediate in the mediation package (72). Models were adjusted for maternal parity and pregnancy weight gain for amniotic fluid IL-6 concentration and kept non-adjusted for maternal serum CRP concentration. Beta-coefficients and SDs or 95% confidence intervals were calculated and are presented in the Results section.

Finally, Pearson correlation tests were applied to assess relationships between expression of all the tested tryptophan pathway genes and inflammatory markers/placental *IL6* gene expression using the rcorr function of the Hmisc package (70). Significant correlation coefficients were represented using an adapted version of the corrplot function of the corrplot package (73).

Supplementary Material

Supplementary Material is available at *HMGJ* online.

Acknowledgements

The authors would like to thank Dr Agnieszka Ciesielska and Dr Antonin Libra for their assistance with qPCR data analysis.

Conflict of Interest statement. The authors declare no conflicts of interest.

Funding

Czech Health Research Council (NU20-01-00264); the Grant Agency of Charles University (SVV 2020/260414); and the EFSA-CDN project (CZ.02.1.01/0.0/0.0/16_019/0000841), which is cofunded by the ERDF. M.R. was supported by a Natural Sciences and Engineering Research Council (NSERC) of Canada (RGPIN/06778-2019) awarded to C.V.

References

1. Chawanpaiboon, S., Vogel, J.P., Moller, A.B., Lumbiganon, P., Petzold, M., Hogan, D., Landoulsi, S., Jampathong, N., Kongwattanakul, K., Laopaiboon, M. *et al.* (2019) Global, regional, and national estimates of levels of preterm birth in 2014: a systematic review and modelling analysis. *Lancet Glob. Health*, **7**, e37–e46.
2. Goldenberg, R.L., Culhane, J.F., Iams, J.D. and Romero, R. (2008) Epidemiology and causes of preterm birth. *Lancet*, **371**, 75–84.
3. Romero, R., Dey, S.K. and Fisher, S.J. (2014) Preterm labor: one syndrome, many causes. *Science*, **345**, 760–765.
4. Kacerovsky, M., Musilova, I., Andrys, C., Hornychova, H., Pliskova, L., Kostal, M. and Jacobsson, B. (2014) Prelabor rupture of membranes between 34 and 37 weeks: the intraamniotic inflammatory response and neonatal outcomes. *Am. J. Obstet. Gynecol.*, **210**, 325.e321–325.e310.
5. Saigal, S. and Doyle, L.W. (2008) An overview of mortality and sequelae of preterm birth from infancy to adulthood. *Lancet*, **371**, 261–269.
6. Nosarti, C., Reichenberg, A., Murray, R.M., Cnattingius, S., Lambe, M.P., Yin, L., MacCabe, J., Rifkin, L. and Hultman, C.M. (2012) Preterm birth and psychiatric disorders in young adult life. *Arch. Gen. Psychiatry*, **69**, E1–E8.
7. Staud, F. and Karahoda, R. (2018) Trophoblast: the central unit of fetal growth, protection and programming. *Int. J. Biochem. Cell Biol.*, **105**, 35–40.
8. Bonnin, A. and Levitt, P. (2011) Fetal, maternal, and placental sources of serotonin and new implications for developmental programming of the brain. *Neuroscience*, **197**, 1–7.
9. Goeden, N., Velasquez, J.C. and Bonnin, A. (2013) Placental tryptophan metabolism as a potential novel pathway for the developmental origins of mental diseases. *Transl. Dev. Psychiatry*, **1**, 20593.
10. Bonnin, A., Goeden, N., Chen, K., Wilson, M.L., King, J., Shih, J.C., Blakely, R.D., Deneris, E.S. and Levitt, P. (2011) A transient placental source of serotonin for the fetal forebrain. *Nature*, **472**, 347–350.
11. Lanoix, D., Beghdadi, H., Lafond, J. and Vaillancourt, C. (2008) Human placental trophoblasts synthesize melatonin and express its receptors. *J. Pineal Res.*, **45**, 50–60.
12. Sedlmayr, P., Blaschitz, A. and Stocker, R. (2014) The role of placental tryptophan catabolism. *Front. Immunol.*, **5**, 230–230.
13. Karahoda, R., Abad, C., Horackova, H., Kastner, P., Zaugg, J., Cerveny, L., Kucera, R., Albrecht, C. and Staud, F. (2020) Dynamics of tryptophan metabolic pathways in human placenta and placental-derived cells: effect of gestation age and trophoblast differentiation. *Front. Cell Dev. Biol.*, **8**, 574034.
14. Williams, M., Zhang, Z., Nance, E., Drewes, J.L., Lesniak, W.G., Singh, S., Chugani, D.C., Rangaramanujam, K., Graham, D.R. and Kannan, S. (2017) Maternal inflammation results in altered tryptophan metabolism in rabbit placenta and Fetal brain. *Dev. Neurosci.*, **39**, 399–412.
15. Manuelpillai, U., Ligam, P., Smythe, G., Wallace, E.M., Hirst, J. and Walker, D.W. (2005) Identification of kynurenine

pathway enzyme mRNAs and metabolites in human placenta: up-regulation by inflammatory stimuli and with clinical infection. *Am. J. Obstet. Gynecol.*, **192**, 280–288.
16. Lanoix, D., Guerin, P. and Vaillancourt, C. (2012) Placental melatonin production and melatonin receptor expression are altered in preeclampsia: new insights into the role of this hormone in pregnancy. *J. Pineal Res.*, **53**, 417–425.
17. Carrasco, G., Cruz, M.A., Dominguez, A., Gallardo, V., Miguel, P. and Gonzalez, C. (2000) The expression and activity of monoamine oxidase A, but not of the serotonin transporter, is decreased in human placenta from pre-eclamptic pregnancies. *Life Sci.*, **67**, 2961–2969.
18. Keaton, S.A., Heilman, P., Bryleva, E.Y., Madaj, Z., Krzyzanowski, S., Grit, J., Miller, E.S., Jälmby, M., Kalapotharakos, G., Racicot, K. *et al.* (2019) Altered tryptophan catabolism in placentas from women with pre-eclampsia. *Int J Tryptophan Res*, **12**, 1178646919840321–1178646919840321.
19. Kudo, Y., Boyd, C.A.R., Sargent, I.L. and Redman, C.W.G. (2003) Decreased tryptophan catabolism by placental indoleamine 2,3-dioxygenase in preeclampsia. *Am. J. Obstet. Gynecol.*, **188**, 719–726.
20. Murthi, P., Wallace, E.M. and Walker, D.W. (2017) Altered placental tryptophan metabolic pathway in human fetal growth restriction. *Placenta*, **52**, 62–70.
21. Ranzil, S., Ellery, S., Walker, D.W., Vaillancourt, C., Alfaidy, N., Bonnin, A., Borg, A., Wallace, E.M., Ebeling, P.R., Erwich, J.J. *et al.* (2019) Disrupted placental serotonin synthetic pathway and increased placental serotonin: potential implications in the pathogenesis of human fetal growth restriction. *Placenta*, **84**, 74–83.
22. Murthi, P. and Vaillancourt, C. (2020) Placental serotonin systems in pregnancy metabolic complications associated with maternal obesity and gestational diabetes mellitus. *Biochim. Biophys. Acta Mol. basis Dis.*, **1866**, 165391.
23. Notarangelo, F.M. and Schwarcz, R. (2016) Restraint stress during pregnancy rapidly raises Kynurenic acid levels in mouse placenta and Fetal brain. *Dev. Neurosci.*, **38**, 458–468.
24. Notarangelo, F.M. and Pocivavsek, A. (2017) Elevated kynurenine pathway metabolism during neurodevelopment: implications for brain and behavior. *Neuropharmacology*, **112**, 275–285.
25. Goeden, N., Velasquez, J., Arnold, K.A., Chan, Y., Lund, B.T., Anderson, G.M. and Bonnin, A. (2016) Maternal inflammation disrupts Fetal neurodevelopment via increased placental output of serotonin to the Fetal brain. *J. Neurosci.*, **36**, 6041–6049.
26. Marley, P.B., Robson, J.M. and Sullivan, F.M. (1967) Embryotoxic and teratogenic action of 5-hydroxytryptamine: mechanism of action in the rat. *Br. J. Pharmacol. Chemother.*, **31**, 494–505.
27. Faupel-Badger, J.M., Fichorova, R.N., Allred, E.N., Hecht, J.L., Dammann, O., Leviton, A. and McElrath, T.F. (2011) Cluster analysis of placental inflammatory proteins can distinguish preeclampsia from preterm labor and premature membrane rupture in singleton deliveries less than 28 weeks of gestation. *Am. J. Reprod. Immunol.*, **66**, 488–494.
28. Romero, R., Avila, C., Santhanam, U. and Sehgal, P.B. (1990) Amniotic fluid interleukin 6 in preterm labor. Association with infection. *J. Clin. Invest.*, **85**, 1392–1400.
29. Prins, J.R., Gomez-Lopez, N. and Robertson, S.A. (2012) Interleukin-6 in pregnancy and gestational disorders. *J. Reprod. Immunol.*, **95**, 1–14.
30. Canetta, S., Sourander, A., Surcel, H.M., Hinkka-Yli-Salomäki, S., Leiviskä, J., Kellendonk, C., McKeague, I.W. and Brown, A.S. (2014) Elevated maternal C-reactive protein and increased risk of schizophrenia in a national birth cohort. *Am. J. Psychiatry*, **171**, 960–968.
31. Brown, A.S., Sourander, A., Hinkka-Yli-Salomäki, S., McKeague, I.W., Sundvall, J. and Surcel, H.M. (2014) Elevated maternal C-reactive protein and autism in a national birth cohort. *Mol. Psychiatry*, **19**, 259–264.
32. Rudolph, M.D., Graham, A.M., Feczko, E., Miranda-Dominguez, O., Rasmussen, J.M., Nardos, R., Entringer, S., Wadhwa, P.D., Buss, C. and Fair, D.A. (2018) Maternal IL-6 during pregnancy can be estimated from newborn brain connectivity and predicts future working memory in offspring. *Nat. Neurosci.*, **21**, 765–772.
33. Smith, S.E.P., Li, J., Garbett, K., Mirnics, K. and Patterson, P.H. (2007) Maternal immune activation alters Fetal brain development through Interleukin-6. *J. Neurosci.*, **27**, 10695–10702.
34. Fricke, E.M., Elgin, T.G., Gong, H., Reese, J., Gibson-Corley, K.N., Weiss, R.M., Zimmerman, K., Bowdler, N.C., Kalantera, K.M., Mills, D.A. *et al.* (2018) Lipopolysaccharide-induced maternal inflammation induces direct placental injury without alteration in placental blood flow and induces a secondary fetal intestinal injury that persists into adulthood. *Am. J. Reprod. Immunol.*, **79**, e12816.
35. Hsiao, E.Y. and Patterson, P.H. (2011) Activation of the maternal immune system induces endocrine changes in the placenta via IL-6. *Brain Behav. Immun.*, **25**, 604–615.
36. Zaretsky, M.V., Alexander, J.M., Byrd, W. and Bawdon, R.E. (2004) Transfer of inflammatory cytokines across the placenta. *Obstet. Gynecol.*, **103**, 546–550.
37. Malek, A., Bersinger, N.A., Di Santo, S., Mueller, M.D., Sager, R., Schneider, H., Ghezzi, F., Karousou, E., Passi, A., De Luca, G. *et al.* (2006) C-reactive protein production in term human placental tissue. *Placenta*, **27**, 619–625.
38. Kim, E.N., Yoon, B.H., Jeon, E.J., Lee, J.B., Hong, J.S., Lee, J.Y., Hwang, D., Kim, K.C., Kim, J.S. and Kim, C.J. (2015) Placental deposition of C-reactive protein is a common feature of human pregnancy. *Placenta*, **36**, 704–707.
39. Romero, R., Espinoza, J., Gonçalves, L.F., Kusanovic, J.P., Friel, L.A. and Nien, J.K. (2006) Inflammation in preterm and term labour and delivery. *Semin. Fetal Neonatal Med.*, **11**, 317–326.
40. Brown, A.G., Tulina, N.M., Barila, G.O., Hester, M.S. and Elovitz, M.A. (2017) Exposure to intrauterine inflammation alters metabolomic profiles in the amniotic fluid, fetal and neonatal brain in the mouse. *PLoS One*, **12**, e0186656.
41. Fukui, S., Schwarcz, R., Rapoport, S.I., Takada, Y. and Smith, Q.R. (1991) Blood-brain barrier transport of kynurenines: implications for brain synthesis and metabolism. *J. Neurochem.*, **56**, 2007–2017.
42. Karahoda, R., Horackova, H., Kastner, P., Matthios, A., Cerveny, L., Kucera, R., Kacerovsky, M., Duintjer Tebbens, J., Bonnin, A., Abad, C. *et al.* (2020) Serotonin homeostasis in the materno-foetal interface at term: role of transporters (SERT/SLC6A4 and OCT3/SLC22A3) and monoamine oxidase A (MAO-A) in uptake and degradation of serotonin by human and rat term placenta. *Acta Physiol.*, **229**, e13478.
43. Masson, J. and Hamon, M. (2009) In Squire, L.R. (ed), *Encyclopedia of Neuroscience*. Academic Press, Oxford, pp. 921–929.
44. Kelly, R., Holzman, C., Senagore, P., Wang, J., Tian, Y., Rahbar, M.H. and Chung, H. (2009) Placental vascular pathology findings and pathways to preterm delivery. *Am. J. Epidemiol.*, **170**, 148–158.

45. Weckman, A.M., Ngai, M., Wright, J., McDonald, C.R. and Kain, K.C. (2019) The impact of infection in pregnancy on placental vascular development and adverse birth outcomes. *Front. Microbiol.*, **10**, 1924–1924.
46. Ranzil, S., Walker, D.W., Borg, A.J., Wallace, E.M., Ebeling, P.R. and Murthi, P. (2019) The relationship between the placental serotonin pathway and fetal growth restriction. *Biochimie*, **161**, 80–87.
47. Riley, L.A., Waguespack, M.A. and Denney, R.M. (1989) Characterization and quantitation of monoamine oxidases A and B in mitochondria from human placenta. *Mol. Pharmacol.*, **36**, 54–60.
48. Auda, G.R., Kirk, S.H., Billett, M.A. and Billett, E.E. (1998) Localization of monoamine oxidase mRNA in human placenta. *J. Histochem. Cytochem.*, **46**, 1393–1400.
49. van Baaren, G.J., Vis, J.Y., Wilms, F.F., Oudijk, M.A., Kwee, A., Porath, M.M., Oei, G., Scheepers, H.C.J., Spaanderman, M.E.A., Bloemenkamp, K.W.M. *et al.* (2014) Predictive value of cervical length measurement and fibronectin testing in threatened preterm labor. *Obstet. Gynecol.*, **123**, 1185–1192.
50. Stranik, J., Kacerovsky, M., Soucek, O., Kolackova, M., Musilova, I., Pliskova, L., Bolehovska, R., Bostik, P., Matulova, J., Jacobsson, B. *et al.* (2021) IgGFc-binding protein in pregnancies complicated by spontaneous preterm delivery: a retrospective cohort study. *Sci. Rep.*, **11**, 6107.
51. Kacerovsky, M., Pliskova, L., Bolehovska, R., Gerychova, R., Janku, P., Matlak, P., Simetka, O., Faist, T., Mls, J., Vescicik, P. *et al.* (2020) Lactobacilli-dominated cervical microbiota in women with preterm prelabor rupture of membranes. *Pediatr. Res.*, **87**, 952–960.
52. Chaemsaithong, P., Romero, R., Korzeniewski, S.J., Martinez-Varea, A., Dong, Z., Yoon, B.H., Hassan, S.S., Chaiworapongsa, T. and Yeo, L. (2016) A rapid interleukin-6 bedside test for the identification of intra-amniotic inflammation in preterm labor with intact membranes. *J. Matern. Fetal Neonatal Med.*, **29**, 349–359.
53. Chaemsaithong, P., Romero, R., Korzeniewski, S.J., Martinez-Varea, A., Dong, Z., Yoon, B.H., Hassan, S.S., Chaiworapongsa, T. and Yeo, L. (2016) A point of care test for interleukin-6 in amniotic fluid in preterm prelabor rupture of membranes: a step toward the early treatment of acute intra-amniotic inflammation/infection. *J. Matern. Fetal Neonatal Med.*, **29**, 360–367.
54. Musilova, I., Andrys, C., Holeckova, M., Kolarova, V., Pliskova, L., Drahosova, M., Bolehovska, R., Pilka, R., Huml, K., Cobo, T. *et al.* (2020) Interleukin-6 measured using the automated electrochemiluminescence immunoassay method for the identification of intra-amniotic inflammation in preterm prelabor rupture of membranes. *J. Matern. Fetal Neonatal Med.*, **33**, 1919–1926.
55. Kacerovsky, M., Tothova, L., Menon, R., Vlkova, B., Musilova, I., Hornychova, H., Prochazka, M. and Celec, P. (2015) Amniotic fluid markers of oxidative stress in pregnancies complicated by preterm prelabor rupture of membranes. *J. Matern. Fetal Neonatal Med.*, **28**, 1250–1259.
56. Salafia, C.M., Weigl, C. and Silberman, L. (1989) The prevalence and distribution of acute placental inflammation in uncomplicated term pregnancies. *Obstet. Gynecol.*, **73**, 383–389.
57. Xie, F., Sun, G., Stiller, J.W. and Zhang, B. (2011) Genome-wide functional analysis of the cotton transcriptome by creating an integrated EST database. *PLoS One*, **6**, e26980.
58. Silver, N., Best, S., Jiang, J. and Thein, S.L. (2006) Selection of housekeeping genes for gene expression studies in human reticulocytes using real-time PCR. *BMC Mol. Biol.*, **7**, 33.
59. Pfaffl, M.W., Tichopad, A., Prgomet, C. and Neuvians, T.P. (2004) Determination of stable housekeeping genes, differentially regulated target genes and sample integrity: BestKeeper—excel-based tool using pair-wise correlations. *Biotechnol. Lett.*, **26**, 509–515.
60. Vandesompele, J., De Preter, K., Pattyn, F., Poppe, B., Van Roy, N., De Paepe, A. and Speleman, F. (2002) Accurate normalization of real-time quantitative RT-PCR data by geometric averaging of multiple internal control genes. *Genome Biol.*, **3**, research0034.1.
61. Andersen, C.L., Jensen, J.L. and Ørntoft, T.F. (2004) Normalization of real-time quantitative reverse transcription-PCR data: a model-based variance estimation approach to identify genes suited for normalization, applied to bladder and colon cancer data sets. *Cancer Res.*, **64**, 5245–5250.
62. Bustin, S.A., Benes, V., Garson, J.A., Hellemans, J., Huggett, J., Kubista, M., Mueller, R., Nolan, T., Pfaffl, M.W., Shipley, G.L. *et al.* (2009) The MIQE guidelines: minimum information for publication of quantitative real-time PCR experiments. *Clin. Chem.*, **55**, 611–622.
63. Bustin, S.A., Benes, V., Garson, J.A., Hellemans, J., Huggett, J., Kubista, M., Mueller, R., Nolan, T., Pfaffl, M.W., Shipley, G.L. *et al.* (2011) Primer sequence disclosure: a clarification of the MIQE guidelines. *Clin. Chem.*, **57**, 919–921.
64. Fox, J. and Weisberg, S. (2018) *An R Companion to Applied Regression*. SAGE Publications.
65. Wickham, H. (2016) *ggplot2: Elegant Graphics for Data Analysis*. Springer-Verlag, New York.
66. Kolde, R. (2019) *R Package Version 1.0.12*.
67. Josse, J. and Husson, F. (2016) missMDA: a package for handling missing values in multivariate data analysis. **70**, 31.
68. Lê, S., Josse, J. and Husson, F. (2008) FactoMineR: an *R package* for multivariate analysis. **25**, 18.
69. Kassambara, A. and Mundt, F. (2020) *R Package Version 1.0.7*.
70. Harrell, F.E.J. (2020) *R Package Version 4.4–1*.
71. Kuhn, M., Jackson, S. and Cimentada, J. (2020) *R Package Version 0.4.2*.
72. Tingley, D., Yamamoto, T., Hirose, K., Keele, L. and Imai, K. (2014) Mediation: *R package* for causal mediation analysis. **59**, 38.
73. Wei, T. and Simko, V. (2017) *R Package "Corrplot": Visualization of a Correlation Matrix (Version 0.84)*.